Supporting Information

Characterization of water-soluble brown carbon chromophores from wildfire plumes in the western USA using size exclusion chromatography

Lisa Azzarello[1], Rebecca A. Washenfelder[2], Michael A. Robinson[2,3], Alessandro Franchin[2,3,4], Caroline Womack[2,3], Christopher D. Holmes[5], Steven S. Brown[2,6], Ann Middlebrook[2], Tim Newberger[7], Colm Sweeney[7], Cora Young[1]

[1]Department of Chemistry, York University, Toronto, ON, M3J 1P3, Canada

[2]Chemical Sciences Laboratory, National Oceanic and Atmospheric Administration, 325 Broadway, Boulder, CO 80305, USA

[3]Cooperative Institute for Research in Environmental Sciences (CIRES), University of Colorado, Boulder, CO, 80309, USA

[4]Now at: National Center for Atmospheric Research, Boulder, CO, USA

[5]Earth, Ocean, and Atmospheric Science, Florida State University, Tallahassee, FL 32304, USA

[6]Department of Chemistry, University of Colorado Boulder, Boulder, Colorado, USA

[7]Global Monitoring Laboratory, National Oceanic and Atmospheric Administration, 325 Broadway, Boulder, CO 80305, USA

Contents:

Figure S5. Absorption density as a function of molecular weight of aqueous samples collected during FIREX-AQ water samples and Suwannee River humic acid. The mobile phase is equal parts acetonitrile and 18.2 MΩ·cm deionized water with 25 mM ammonium acetate at a flow rate of 1 mL min^{-1}.

Figure S6. Total absorption at 365 nm to CO as a function of plume age of water extracts for smoke sampled of glass microfiber filters in Vancouver (Di Lorenzo et al. 2017) The green and blue squares represent absorption at 365 nm to CO of water extracts sampled on Teflon filters aboard the NASA DC-8 aircraft during SEAC4RS (Forrister et al. 2015)

Figure S7. Absorption contribution of high (>500 Da), low (<500 Da), and unidentified molecular weight species of aqueous samples collected during (a) 24 Aug 2019, (b) 25 Aug 2019 L2, (c) 28 Aug 2019 L1, (d)) 28 Aug 2019 L2, and (e)) 28 Aug 2019 L3.

Table S1: Summary of flights completed by the NOAA "Chemistry" Twin Otter aircraft during FIREX-AQ 2019.

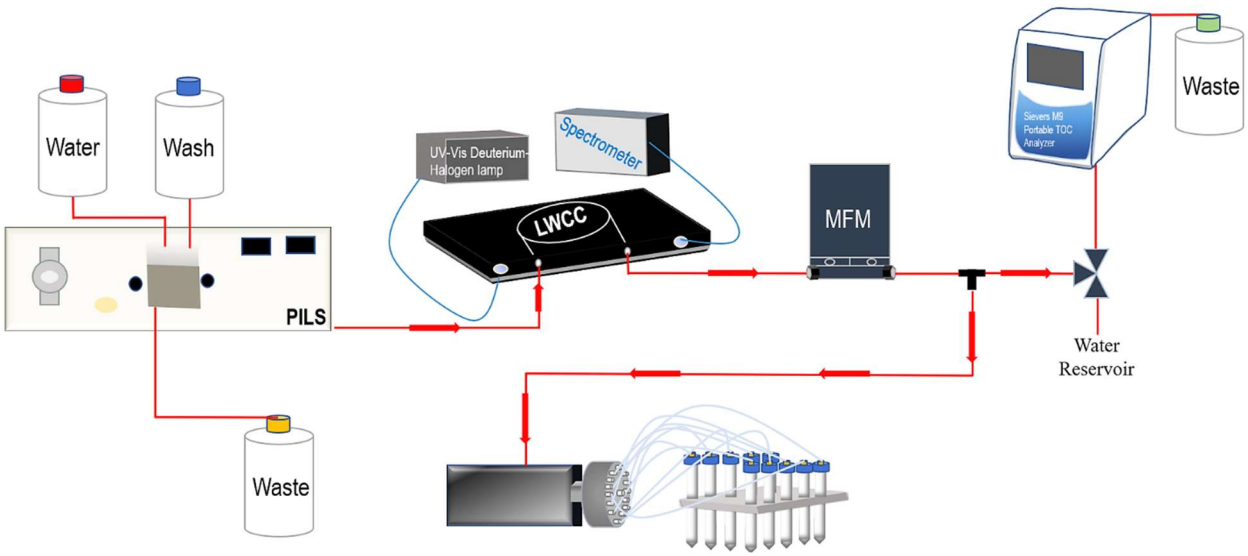

Figure S1. A schematic showing the liquid flow within the BrC-PILS. MFM is liquid mass flow meter and LWCC is liquid waveguide capillary cell.

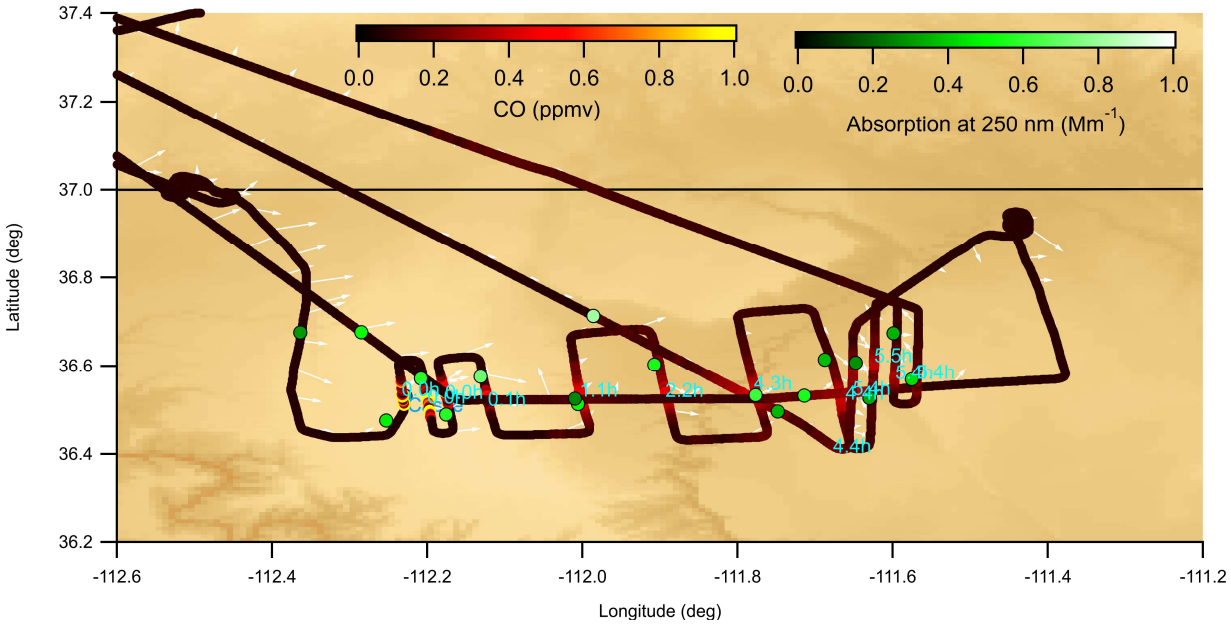

Figure S2. Selected map of second flight on 21 Aug 2019 of the Castle fire. The circular markers are coloured by absorption at 250 nm measured by SEC-UV and represent the average location where liquid flow was diverted into a single polypropylene sample tube.

Text S1: Mobile phase impact on SEC-UV elution profile

Analysis by SEC-UV allows us to examine the molecular size of BrC chromophores as a function of plume age. As the mobile phase carries the sample through the porous stationary phase of a SEC column, high MW molecules that exceed the size of the pores will flow directly

through the column, passing the pores. This will result in an early elution time within the void volume. If absorbing species are small enough to penetrate the pores, they will spend more time in the column and elute later. All molecules that are smaller than the limit to fully penetrate the pores of the stationary phase will elute in the exclusion volume. Figure S3 displays single-wave size-exclusion chromatogram at 250 nm for aqueous samples collected on 21 Aug 2019. The absorption density of the aqueous samples listed in Table S1 had consistent size-resolved features with varying magnitude in absorption. The first peak between 8.5 to 9 minutes is characteristic of relatively higher MW compounds than the second peak between 9.5 to 11.

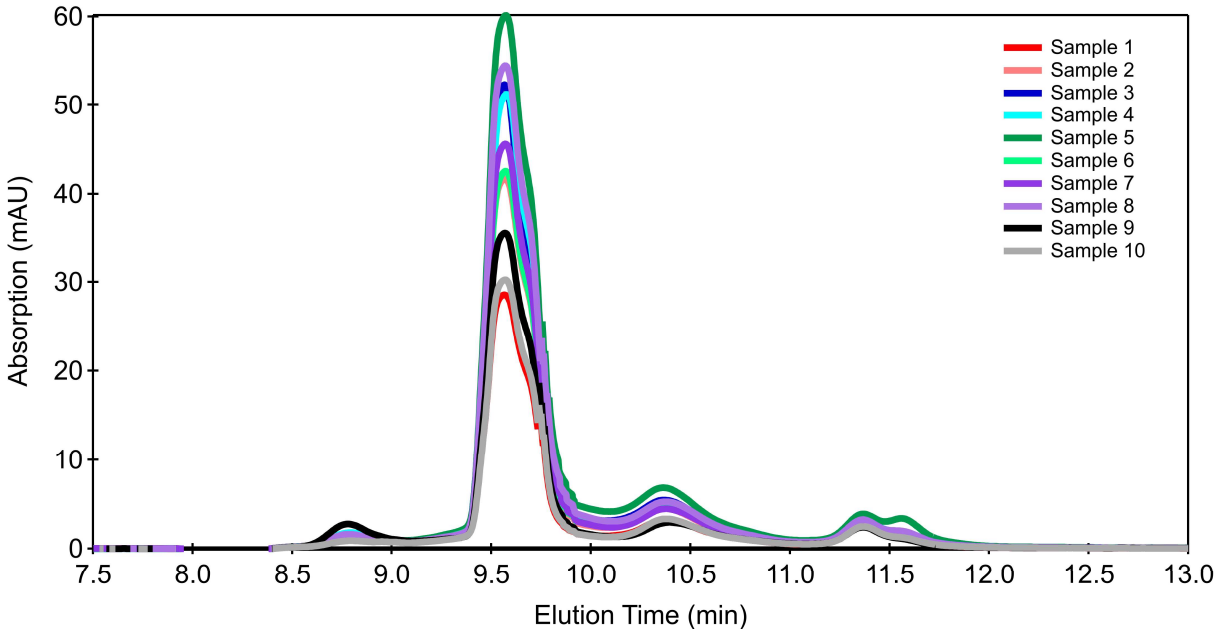

Figure S3. Example of absorption density plot at 250 nm of FIREX-AQ aqueous samples collected during the second flight 21 Aug 2019, of the Castle fire. The mobile phase is equal parts acetonitrile and 18.2 MΩ·cm deionized water with 25 mM ammonium acetate at a flow rate of 1 mL min^{-1}.

Figure S4 displays single-wavelength size-exclusion chromatograms of an aqueous separation on the SEC-UV with varying mobile phase compositions. With equal parts methanol and buffer solution, the low MW fractions eluted after exclusion volume of the SEC column (<250 Da). With the addition of acetonitrile, it appears that the apparent higher MW fraction then co-eluted with the low MW fraction (represented by a single peak in the orange trace; Figure S4). Similar to the findings of Lyu et al. (2021) using equal parts acetonitrile and buffer solution appears to be effective in suppressing interactions between the stationary phase of the SEC column and chromophores, as a narrow elution profile of a low MW fraction was observed.

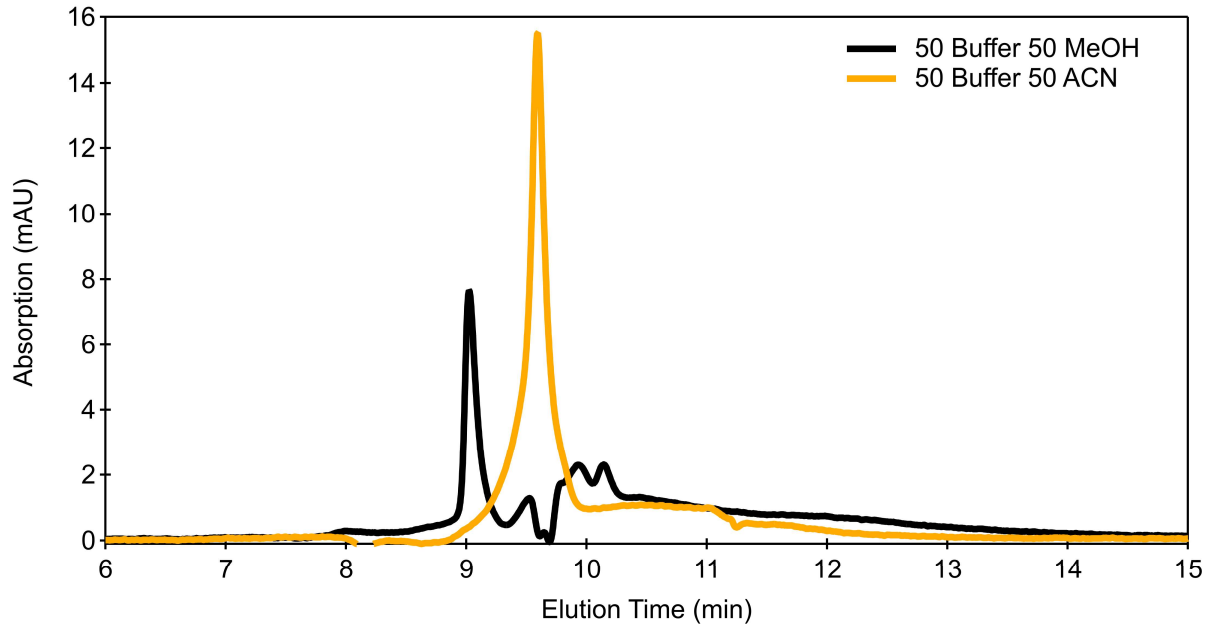

Figure S4: Single-wavelength chromatogram at 250 nm of an aqueous sample run with equal parts buffer solution and methanol (black) and equal parts buffer solution and acetonitrile (orange)

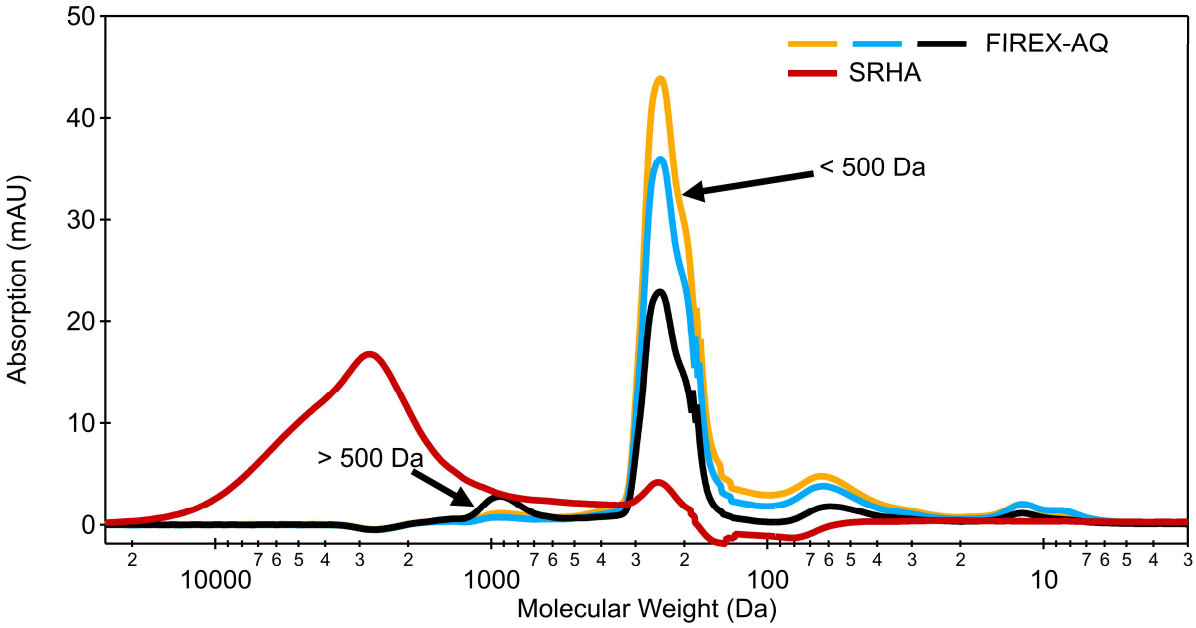

Figure S5. Absorption density as a function of molecular weight of aqueous samples collected during FIREX-AQ water samples and Suwannee River humic acid. The mobile phase is equal parts acetonitrile and 18.2 MΩ·cm deionized water with 25 mM ammonium acetate at a flow rate of 1 mL min^{-1}.

Text S2: Conversion of SEC-UV signal to ambient absorption units of Mm^{-1}

To compare absorption of the water soluble BrC measured online by the BrC-PILS, the absorption data measured by SEC-UV was converted to inverse megameters, Mm^{-1}. The absorption of different MW fractions at a selected wavelength is determined by integrating the peak area. To apply the Beer-Lambert Law to the absorption profiles by the SEC-UV method, the dilution of the sample during this analysis must be considered. The absorbance of the sample, A_λ, is a function of injection volume, V_i, and the absorbance across a peak, $A_{\lambda p}$, is dependent on the volume across a peak, V_p. The value of V_p can be determined by multiplying the flow rate by the peak width. The peak area, a_p, is the product of the absorbance intensity (mAU) multiplied by the peak width (minutes), w_p.

Absorbance across a peak	Absorbance of sample collected
$A_{\lambda p} = \varepsilon\ l\ c_p$ $A_{\lambda p} = \varepsilon\ l\ n/V_p$ $\varepsilon = A_{\lambda p} \cdot V_p / l\ n$	$A_\lambda = \varepsilon\ l\ c$ $A_\lambda = \varepsilon\ l\ n/V_i$ $\varepsilon = A_\lambda \cdot V_i / l\ n$
$A_{\lambda p} = A_\lambda \cdot V_i / V_p$ Eq (1)	
Volume across peak $a_p = A_{\lambda p} \cdot w_p$ $w_p = V_p / F$ **$A_{\lambda p} = a_p \cdot F / V_p$ Eq (2)** **Combine Eq 1 & 2** $a_p \cdot F / V_p = A_\lambda \cdot V_i / V_p$ $a_p \cdot F = A_\lambda \cdot V_i$ **$A_\lambda = a_p \cdot F / V_i$ Eq (3)**	

For this analysis, the conversion of the absorbance (mAU) of a water sample (A_λ) to Mm^{-1} considers the volume collected by the PILS and the volume of air sampled by the inlet system as described in Washenfelder et al. (2022), and the PILS collection efficiency:

$$\text{Absorption}(\text{Mm}^{-1}) = \frac{\text{peak area} \times \text{SEC Flow rate}}{\text{Injection Volume}} \times \frac{\text{PILS Flow}}{\text{Gas flow} \times \text{Optical path}} \times \ln(10) \times \text{PILSCollectionEff}$$

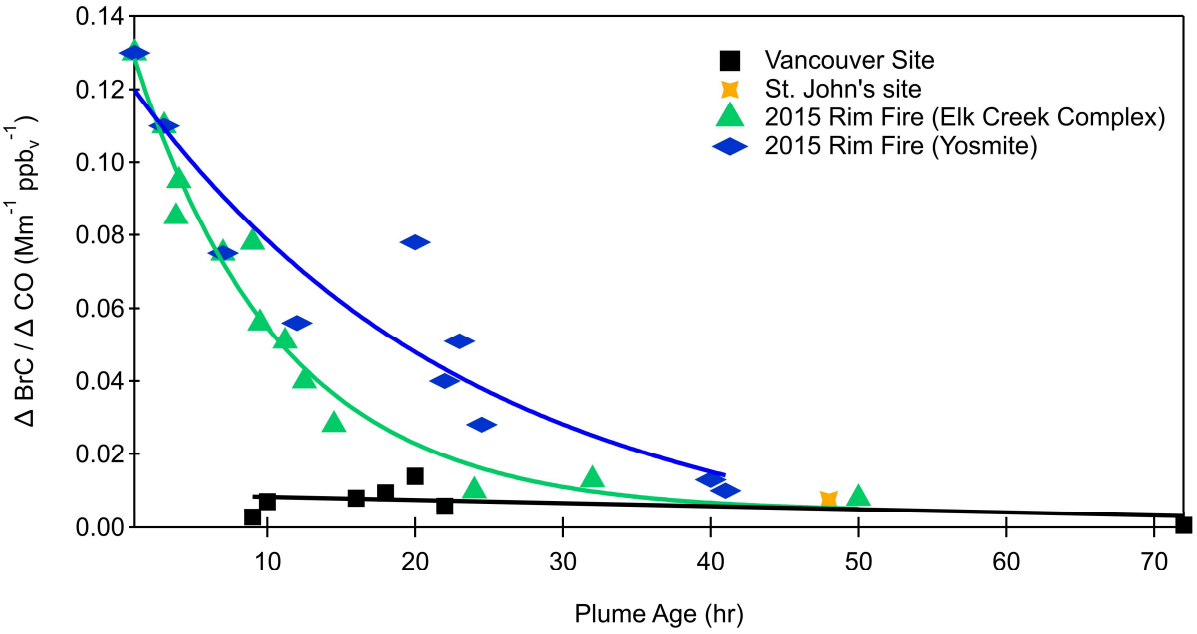

Figure S6. Absorption at 365 nm to CO as a function of plume age of water extracts for smoke sampled of glass microfiber filters in Vancouver (Di Lorenzo et al., 2017) The green and blue squares represent absorption at 365 nm to CO of water extracts sampled on Teflon filters aboard the NASA DC-8 aircraft during SEAC4RS (Forrister et al. 2015).

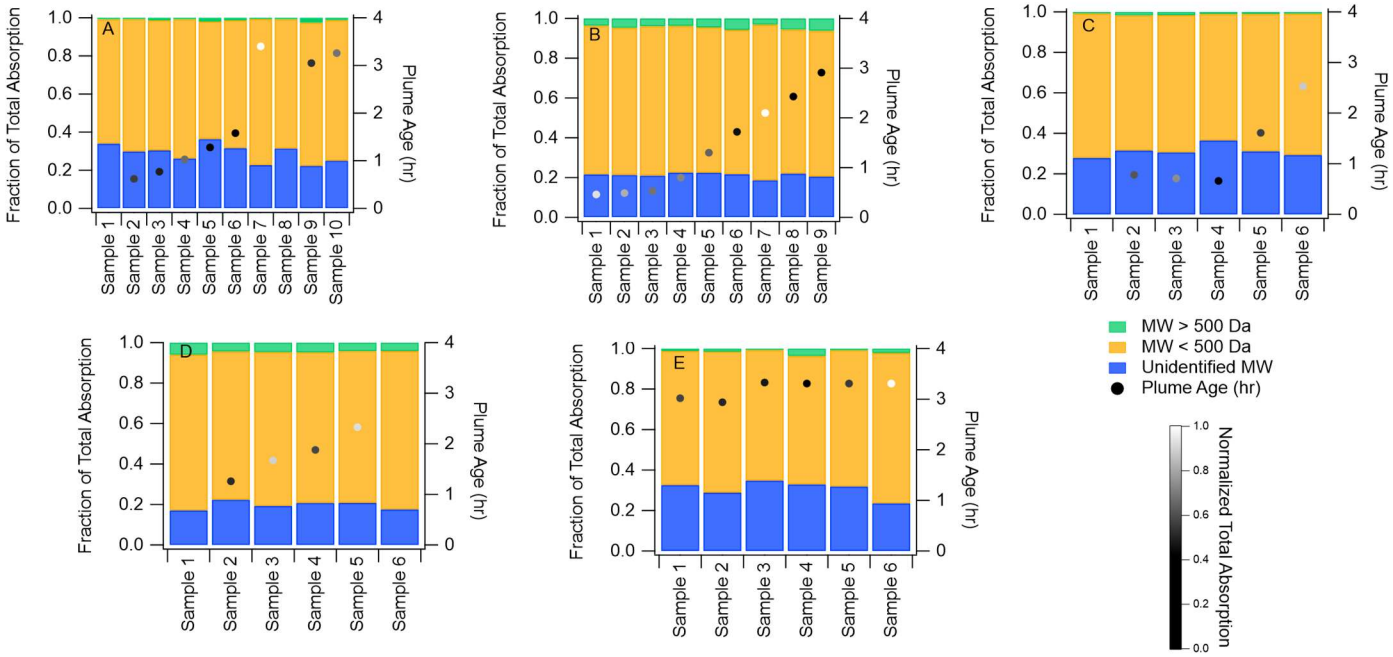

Figure S7. Absorption contribution of high (>500 Da), low (<500 Da), and unidentified molecular weight species of aqueous samples collected during (a) 24 Aug 2019, (b) 25 Aug 2019 L2, (c) 28 Aug 2019 L1, (d)) 28 Aug 2019 L2, and (e)) 28 Aug 2019 L3.

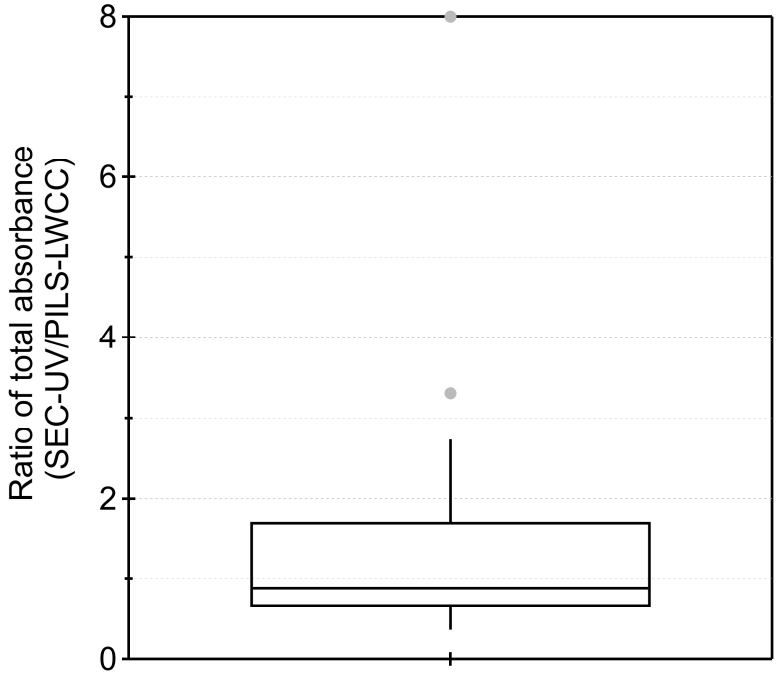

Figure S8. Relationship between BrC absorption as measured by SEC−UV offline and by PILS−LWCC online during the Southern Oxidant and Aerosol Study (SOAS) in the Talladega National Forest in Alabama, USA. Offline samples were collected on a filter assembly of a broadband cavity enhanced spectrophotometer and online particle absorption was measured using a PILS-LWCC (Di Lorenzo et al., 2017).

Table 1. Summary of flights completed by the NOAA "Chemistry" Twin Otter aircraft during FIREX-AQ 2019.

US State	Fire Name	Fuel	Date and Flight leg	Number of water samples collected	Number of Transects	Plume age range (hr)
Arizona	Castle	Grassland, timber, mixed conifer	20190821-L2	10	8	0.2 – 4.1
Oregon	204 Cow	Sub-alpine fir, timber, grass	20190824-L2	10	8	0.5 – 2.4
			20190825-L2	9	10	0.5 – 2.9
			20190828-L1	6	6	0.7 – 1.8
			20190828-L2	6	4	1.3 – 2.9
			20190828-L3	6	4	2.2 – 4.2

References

Di Lorenzo, R. A., Washenfelder, R. A., Attwood, A. R., Guo, H., Xu, L., Ng, N. L., Weber, R. J., Baumann, K., Edgerton, E., and Young, C. J.: Molecular-size-separated brown carbon absorption for biomass-burning aerosol at multiple field sites, Environmental Science and Technology, 51, 3128–3137, https://doi.org/10.1021/acs.est.6b06160, 2017.

Forrister, H., Liu, J., Scheuer, E., Dibb, J., Ziemba, L., Thornhill, K. L., Anderson, B., Diskin, G., Perring, A. E., Schwarz, J. P., Campuzano-Jost, P., Day, D. A., Palm, B. B., Jimenez, J. L., Nenes, A., and Weber, R. J.: Evolution of brown carbon in wildfire plumes, Geophysical Research Letters, 42, 4623–4630, https://doi.org/10.1002/2015GL063897, 2015

Lyu, M., Thompson, D. K., Zhang, N., Cuss, C. W., Young, C. J., and Styler, S. A.: Unraveling the complexity of atmospheric brown carbon produced by smoldering boreal peat using size-exclusion chromatography with selective mobile phases, Environ. Sci.: Atmos., 1, 241–252, https://doi.org/10.1039/D1EA00011J, 2021.